

Benchmarking quantum mechanical calculations with experimental NMR chemical shifts of 2-HADNT



Yuemin Liu^a, Thomas Junk^a, Yucheng Liu^{b,*}, Nianfeng Tzeng^c, Richard Perkins^a

^a Department of Chemistry, University of Louisiana at Lafayette, Lafayette, LA 70504, USA

^b Department of Mechanical Engineering, Mississippi State University, Mississippi State, MS 39762, USA

^c The Center for Advanced Computer Studies, University of Louisiana at Lafayette, Lafayette, LA 70504, USA

HIGHLIGHTS

- Chemical shifts of C-13 of seven carbon atoms for 2-HADNT were determined through experiments.
- Quantum mechanics GIAO calculations were implemented using MP2 and seven DFT methods.
- It was found that the O3LYP method gives the most accurate chemical shift values among the seven DFT methods.
- Three types of atomic partial charges MK, ESP and NBO were calculated using MP2/aug-cc-pVDZ method.
- Numerical calculations of NMR chemical shifts were validated by comparing with the experimental data.

ARTICLE INFO

Article history:

Received 19 November 2014

Received in revised form 2 January 2015

Accepted 5 January 2015

Available online 9 January 2015

Keywords:

Quantum mechanical calculations

Chemical shifts

Partial charges

NMR

2-HADNT

C-13

ABSTRACT

In this study, both GIAO-DFT and GIAO-MP2 calculations of nuclear magnetic resonance (NMR) spectra were benchmarked with experimental chemical shifts. The experimental chemical shifts were determined experimentally for carbon-13 (C-13) of seven carbon atoms for the TNT degradation product 2-hydroxylamino-4,6-dinitrotoluene (2-HADNT). Quantum mechanics GIAO calculations were implemented using *Becke-3-Lee-Yang-Parr* (B3LYP) and other six hybrid DFT methods (*Becke-1-Lee-Yang-Parr* (B1LYP), *Becke-half-and-half-Lee-Yang-Parr* (BH and HLYP), *Cohen-Handy-3-Lee-Yang-Parr* (O3LYP), *Coulomb-attenuating-B3LYP* (CAM-B3LYP), modified-Perdew-Wang-91-*Lee-Yang-Parr* (mPW1LYP), and *Xu-3-Lee-Yang-Parr* (X3LYP)) which use the same correlation functional LYP. Calculation results showed that the GIAO-MP2 method gives the most accurate chemical shift values, and O3LYP method provides the best prediction of chemical shifts among the B3LYP and other five DFT methods. Three types of atomic partial charges, Mulliken (MK), electrostatic potential (ESP), and natural bond orbital (NBO), were also calculated using MP2/aug-cc-pVDZ method. A reasonable correlation was discovered between NBO partial charges and experimental chemical shifts of carbon-13 (C-13).

© 2015 Elsevier B.V. All rights reserved.

Introduction

Reliability of theoretical calculations has been recognized in predicting nuclear magnetic resonance (NMR) shielding and chemical shifts [1–8]. Accurate prediction of chemical shifts can be achieved through calculations using the coupled-cluster singles and doubles (CCSD) model augmented by perturbative correction for triple excitation (CCSD(T)) method [9–11], with a deviation of 1 ppm between the experimental chemical shifts and the calculated results for C-13. The accuracy can be further improved by the inclusion of zero-point vibrational correction in the

Hartree-Fock (HF), MP2, CCSD, and CCSD(T) calculations of the chemical shifts except for the DFT calculations [11].

The gauge that includes atomic orbital (GIAO) was first implemented with $X-\alpha$ approximation of the exchange-correlation functional (DFT) [12,13]. The second-order property shielding tensor has also been described using other methods such as the individual gauge for localized orbitals (IGLO) [14,15], the individual gauge for local origin (LORG) [16], the continuous set of gauge transformations (CSGT) [17], and the individual gauges for atoms in molecules (IGAIM) [18]. Among these methods, the GIAO method is most commonly applied because of its high efficiency and low dependence on basis set quality [19].

The chemical shifts for C-13 have been calculated using wave function based methods such as MP2 [20–22], multi-configurational self-consistent field (MCSCF) [22,23], CCSD

* Corresponding author.

[24,25], CCSD(T) [26], and coupled cluster theory with single, double, and triple excitations (CCSDT) [27,28]. However, the computational cost of those methods is so high, which prevents full application of those methods for routine simulations. The DFT methods are more cost-effective approaches because that in those methods electron correlation is treated at a more affordable semi-empirical level. The C-13 chemical shift calculated from DFT methods such as GIAO and B3LYP can provide structural information for different charge states [29]. On the other hand, the experimental C-13 chemical shifts can be well reproduced using B3LYP for monomeric bilirubin molecule [30]. It is also known that DFT methods generate much more accurate geometries and potential energy profiles than HF method at a similar computational expense. Unfortunately, DFT methods could not demonstrate decisive superiority over HF method in the calculations of chemical shifts of all types of compounds. DFT methods are different based on different exchange–correlation functionals (XC) implemented and the different DFT methods used may lead to different accuracies in the calculated chemical shifts [31]. Additionally, DFT methods tend to provide lower chemical shifts for regular organic compounds but higher chemical shifts for transition metals than their actual values because the paramagnetic components are overestimated in non-transition metal compounds while underestimated in the compounds containing transition metals [32]. The deficiency in the chemical shifts prediction is due to the lack of terms that describe non-vanishing electric current in popular DFT methods [33], the underestimation of the highest and lowest unoccupied molecular orbital (HOMO–LUMO) gap, as well as the unrealistic larger paramagnetic values than their experimental results for the regular organic compounds that contain no transition metals [34,35]. Currently, calculations of chemical shifts can be performed at fundamental HF level with reasonable accuracy for small weakly correlated organic molecules. Electron correlation has to be fully considered in order to achieve high accuracy on chemical shifts for dispersion dominated large molecules. The DFT treatment of electron correlations varies in how to formulate the following four components: spin density based local density approximation (LDA), a generalized gradient approximation (GGA) for density derivatives, HF exchange, and kinetic energy density terms. For example, the popular DFT method B3LYP represents the combination of a standard LDA, a gradient correction GGA, and the HF exchange [36,37]. It was reported that DFT O3LYP differs from B3LYP in an optimized exchange functional, while performs better than B3LYP in describing van der Waals force in highly correlated molecules [38,39]. One of the goals of this work is to test how the different exchange functionals impact the performance of the seven DFT methods in evaluating chemical shifts of the highly correlated aromatic 2-HADNT. In concept, electronic environments of nuclei in chemical structure determine nuclear chemical shifts or nuclear resonance frequencies [40]. In fact, C-13 chemical shift was suggested to be linearly proportional to electron density. A study of C-13 chemical shift of the cyclopentadienide anion suggested that the proportionality coefficient is 128.5 ppm/electron [41]. A strong correlation was reported between the partial charges calculated by Matsumoto et al. and the experimental chemical shifts of C-13 and N-15 for pyridinium bis (methoxycarbonyl) methylides [42]. For a highly electron correlated molecule, it is especially meaningful in both theory and practice to explore the correlation between the experimental C-13 chemical shifts and electron partial charges and calculated C-13 chemical shifts and electron partial charges respectively for 2-HADNT (Fig. 1) [43]. In this study, both quantum mechanics gauge including atomic orbital-density functional theory (GIAO-DFT) and quantum mechanics gauge including atomic orbital-second order Moller–Plesset perturbation theory (GIAO-MP2) simulations are performed to reproduce experimental C-13 chemical shifts of

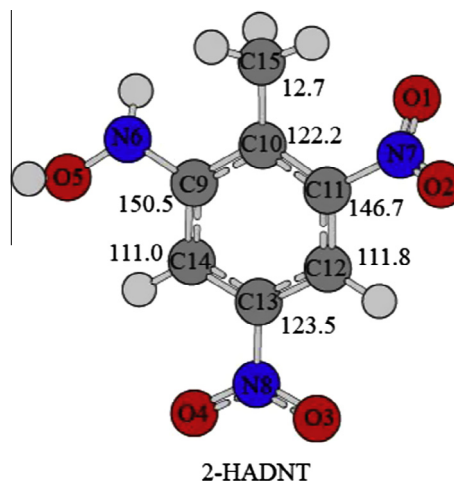


Fig. 1. Schematic structure of 2-HADNT with numbering scheme displayed.

2-HADNT from NMR measurement. From the simulation results, the correlations between the calculated partial charges of C-13 of 2-HADNT and the experimental C-13 chemical shifts can be found. Effects of different exchange functionals on the accuracy of the calculated chemical shifts will also be discussed. All the chemical shifts and partial charges will be calculated using MP2 and the seven DFT methods, compared with the experimental chemical shifts afterwards.

Research approaches

Experimental setup

The 2-HADNT was prepared following the procedure in the authors' previous work [43]. Chloroform (CHCl_3) (analytical purity, made by Merck) was used as a solvent for measurement. Tetramethylsilane (TMS) (made by Fluka) was applied as the internal reference. The C-13 magnetic resonance spectra were recorded at a radio frequency of 500.1 Mc/s on a Varian 500 spectrometer in the Department of Chemistry at the University of Louisiana at Lafayette. The sample of concentration was maintained at 25 ± 1 °C. The effect of proton coupling was removed using a noise decoupling technique.

Computational approach

The chemistry application Gaussian 09 package was used in all computations of this work [44]. Initial crystal structure of 2-HADNT was optimized using MP2/aug-cc-pVDZ. The C-13 NMR calculations were carried out using GIAO method [19]. The NMR shifts were computed using MP2 and seven DFT hybrid methods and the C-13 chemical shifts were referenced to C-13 chemical shifts for TMS using GaussView Version 5. The chemical shift of 128.5 ppm for C-13 of benzene was used to calculate chemical shift differential. The solvation effect of chloroform with a dielectric constant of 4.7 was evaluated using the universal solvation model (SMD) presented by Truhlar et al. [45], which includes electrostatic term based on integral equation formalism polarized continuum model (IEF-PCM) and non-electrostatic cavity–dispersion–solvent–structure term. The NBO charges were computed following the NBO scheme implemented within the Gaussian 09 platform. The basis set of aug-cc-pVDZ was used throughout all calculations.

Results and discussion

Accuracy of calculated chemical shifts

Fig. 1 shows a numbering scheme for naming system of seven carbon atoms. All experimental and calculated chemical shifts (using MP2 method) are listed in Table 1. To account for the discrepancy between experimental and calculated chemical shifts, twisting torsion angles are summarized in Table 2 for 2-NHOH, 4-NO₂, and 6-NO₂ of crystal and optimized structures of 2-HADNT in this work, and Graham and coworkers' study [52]. From Table 1 it can be concluded that the chemical shifts calculated in chloroform and dimethyl sulfoxide (DMSO) are very close to each other, indicating minor effect of the most commonly used solvents on theoretical calculations of chemical shifts. The comparison between the experimental data and the values calculated using MP2/aug-cc-pVDZ method with the chloroform solvation model is displayed in Fig. 2. From that figure it can be seen that the computational results agreed well with the experimental data. Among the presented chemical shifts, C₉, C₁₁, and C₁₅ are most accurately predicted by MP2 calculations with a range of 6.4–1.6 ppm. Moderate deviations of 10.0 ppm from calculations were observed from experimental values for C₁₂ and C₁₄. The largest differences of from 17.2 ppm to 25.8 ppm occur between theoretical and experimental data for C₁₀ and C₁₃. The significant discrepancy of 25.8 ppm at C₁₃ likely results from the rotatable 4-NO₂ group, since energy barrier is only 3.8 kcal/mol from coplanar 4-NO₂ in crystal and optimized structures to the orthogonal 4-NO₂ [53]. Orientation of 4-NO₂ has been proved to be coplanar in our initial crystal structure, opti-

Table 1
Comparison of experimental chemical shifts with calculated chemical shifts using MP2 methods.

Chemical shift (ppm)	C ₉	C ₁₀	C ₁₁	C ₁₂	C ₁₃	C ₁₄	C ₁₅
EXPL (CHCl ₃)	146.7	122.2	150.5	111.8	123.5	111.0	12.7
MP2 (CHCl ₃)	152.8	139.4	153.0	121.4	149.3	121.4	14.3
MP2 (DMSO)	153.1	140.9	152.9	121.4	149.1	121.3	14.5

Table 2
Twisting angles of 2-NHOH, 4-NO₂, and 6-NO₂.

Torsion	Crystal	Crystal ^a	Optimized (MP2/aug-cc-pVDZ)
O5–N7–C9–C10 (2-NHOH)	10.0	10.3	15.0
O4–N8–C10–C11 (4-NO ₂)	2.8	3.24	2.7
O2–N7–C10–C9 (6-NO ₂)	54.3	55.6	46.5

^a This crystal structure is extracted from Graham and co-worker's study deposited in Cambridge Structural Database.

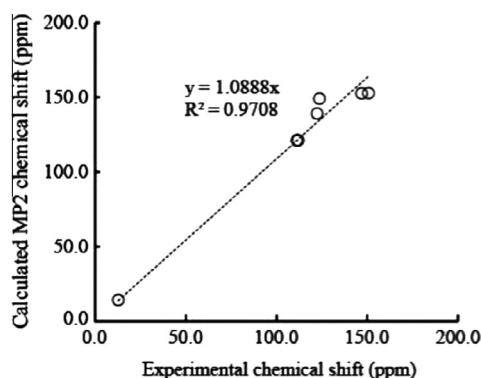


Fig. 2. Correlation between experimental and calculated chemical shifts.

mized structure, and crystal structure in Graham and co-work's study [52]. However, chemical shift for C₁₃ in CHCl₃ solution could be averaged from the dynamic twisting orientations of 4-NO₂ rather than single static coplanar conformer for calculated chemical shift. Similarly, C₁₀ sits in the middle of 2-NHOH, and methyl, and 6-NO₂, and orientations of methyl and 6-NO₂ could be changed constantly in CHCl₃ solution due to the low energy barrier of 1.8 kcal/mol [53]. So variation of twisting angles of methyl and 6-NO₂ could cause fluctuation of electronic environment of C₁₀ and gives rise to the 17.2 ppm differential between calculated and experimental chemical shifts.

Effect of methodology on NMR calculations

Chemical shifts calculated from MP2 and other seven DFT methods are compared and plotted in Figs. 3 and 4. Even the MP2 method offers good accuracy, it is very computational costly and usually requires a large amount of disk space. Therefore, the DFT methods, which are relatively more efficient, are used to be applied for the NMR calculations. DFT methods usually differ in either exchange functional (Ex[P]), or correlation functional (Ec[P]), or combination of the two in the Kohn–Sham formulation. This study only focuses on the DFT methods with different exchange functional but the same correlation functional. Comparing with MP2 method in Fig. 3, B3LYP showed an average deviation of 16.1 ppm from the experimentally measured chemical shifts for the seven C-13 atoms (C₉ to C₁₅) while the largest deviation from MP2 is only 10.5 ppm. Among the seven DFT methods, O3LYP method, which includes Handy's OPTX modification of Becke's exchange functional, provided the best accuracy and its average deviation is 11.2 ppm. With that observation, a detailed comparison was further made among the B3LYP, O3LYP, and the MP2 results, which is shown in Fig. 4. From that figure it is revealed that C₁₀, C₁₂, and C₁₄ calculated from O3LYP are more accurate than those generated from MP2. The best prediction provided by

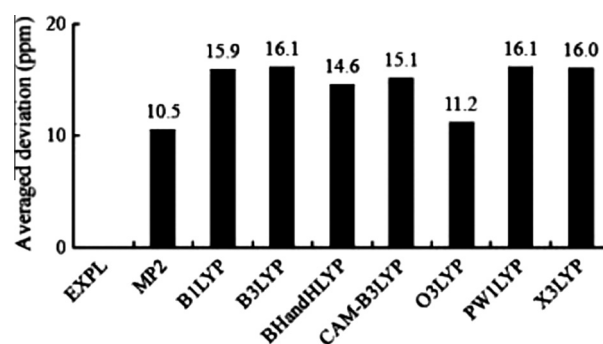


Fig. 3. Method dependence of averaged deviations of calculated chemical shift.

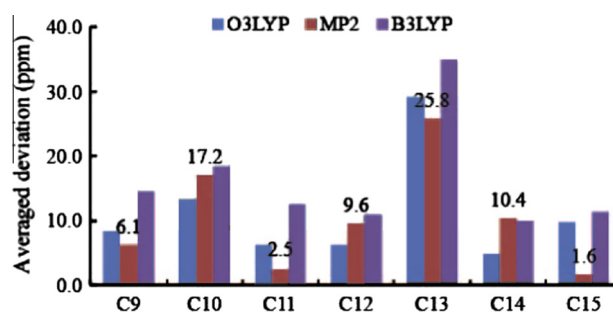


Fig. 4. Detailed comparison of chemical shift of seven carbon atoms.

B3LYP is for C₁₄, but the derivation by B3LYP from the experimental value for C₁₄ is still larger than that by O3LYP. The comparison results verify that with the optimized exchange functional, O3LYP performs better than B3LYP in describing van der Waals force in the highly correlated molecules [38,39], despite B3LYP may outperform O3LYP in the simulations of the first-row of transition metals [6,46–49].

Correlation between calculated partial charge and experimental chemical shifts

The experimental chemical shifts and three types of atomic partial charges, natural bond orbital (NBO), electrostatic potential (ESP), and Mulliken charges (MK) are listed in Table 3. The relationships between the three types of calculated partial charges and the experimental chemical shifts are depicted in Fig. 5. Fig. 5(a) shows the relationship between the absolute chemical shifts and partial charges of all seven carbon atoms; Fig. 5(b) indicates the correlations between the relative chemical shifts of carbon atoms on phenyl ring (with respect to the chemical shifts on benzene ring) and relative partial charges of carbon atoms on phenyl ring (with respect to the relative partial charges of carbon atoms on benzene ring). As also displayed in Fig. 5, the six relationships (absolute and relative chemical shifts vs. three types of absolute and relative charges) are approximated through six developed linear regression models with their coefficients of multiple determination (R²) calculated.

When a magnetic field (B₀) is in place, energy splitting arises from the two energetically degenerate spin states of nuclei with none-zero spin quantum number (such as H-1 and C-13) in molecules. This energy splitting is linearly proportional to the strength of the applied magnetic field B, and can be expressed as:

$$E = h \cdot \nu_0 = h \cdot \gamma \cdot B / 2\pi \quad (1)$$

where h , ν_0 , and γ refer to Planck constant, Larmor precession frequency, and gyromagnetic ratio respectively).

Eq. (1) is then rearranged to solve for Larmor precession frequency as:

$$\nu_0 = \gamma \cdot B / 2\pi \quad (2)$$

It should be noted that the actual magnetic field strengths (B) experienced by nuclei in real molecules vary from nucleus to nucleus depending on their opposing induced magnetic field originated from surrounding electron density. Actual magnetic field strengths should be formulated as:

$$B = B_0 - B_e \quad (3)$$

The strength of the opposing magnetic field can be calculated by:

$$B_e = \frac{\mu_0}{2r} \times I = \frac{\mu_0}{2r} \times \frac{q}{\Delta t} = \frac{\mu_0}{2r} \times \frac{qv}{2\pi r} = \frac{\mu_0 v}{4\pi r^2} \times q_\delta \quad (4)$$

where μ_0 , r , q_δ , and v are magnetic moment, radius of electron orbital, number of electrons associated with the nucleus, and velocity of electrons.

Electron density refers to the probability ($\rho(r)$) of finding electrons at a point (r) within molecules. Electron density implies locations of electrons in molecules, and enables visualization of the molecular size. Electron density can be interpreted as the square of quantum mechanical wave function as:

$$\rho(r) = 2 \sum_{i=1}^{n/2} |\psi_i(r)|^2 \quad (5)$$

where ψ , n , and $n/2$ are molecular orbital, number of electrons, and occupied orbitals.

Integration of electron density over the wave function or basis set for the atom A gives the number of electrons, so the number of electrons associated with atom can be expressed as:

$$\int \rho(r) dr = q_A \quad (6)$$

In quantum mechanics calculations, population analysis mathematically partition electron densities into partial charges on individual atom, and the atomic partial charge (q_δ) is the sum of positive nuclear charge (N) and number negative charge of

Table 3
Experimental chemical shifts and three types of atomic partial using MP2 method.

Carbon	Chemical shift	NBO	ESP	Mulliken
C ₉	146.7	0.19833	0.622247	-0.055720
C ₁₀	122.2	-0.06877	-0.264403	0.185505
C ₁₁	150.5	0.12559	0.196977	0.392160
C ₁₂	111.8	-0.24864	-0.509574	0.760910
C ₁₃	123.5	0.11489	0.225757	0.729585
C ₁₄	111.0	-0.25986	-0.484148	0.946413
C ₁₅	12.7	-0.64596	-0.226587	0.506832

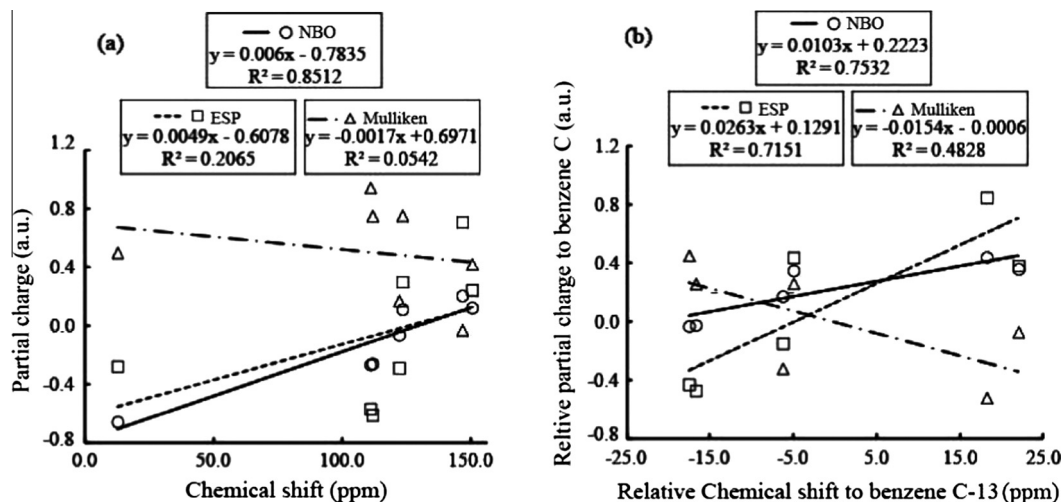


Fig. 5. Relationships between three types of calculated partial charges and experimental chemical shifts (a) relationship between absolute chemical shifts and absolute partial charges of all seven carbon atoms; and (b) correlations between relative chemical shifts to benzene ring and relative partial charges to benzene ring.

electrons associated with the nucleus (q_A), and so the number negative charge of electrons associated with the nucleus (q_A) can be calculated as following:

$$(q_A = N - q_\delta) \quad (7)$$

Arbitrary method can be employed to calculate the partial charge since it is not a quantum mechanically observable property. In NMR, all experimental frequencies are referenced against TMS, and the chemical shift is numerically proportional to partial charge on the nucleus and can be defined as:

$$\delta = \frac{\nu_0 - \nu_{\text{TMS}}}{\nu_{\text{NMR}}} \quad (8)$$

where ν_0 and ν_{TMS} are the Larmor precession frequency for sample and TMS respectively.

Thus, Eqs. (2)–(4), (7) and (8) can be combined to achieve the simplified expression

$$\delta = \frac{\nu_0 - \nu_{\text{TMS}}}{\nu_{\text{NMR}}} = \frac{\gamma(B_0 - \frac{\mu_0 \nu}{4\pi r^2}(N - q_\delta)) - \nu_{\text{TMS}}}{\nu_{\text{NMR}}} = a \times q_\delta + b \quad (9)$$

where $a = \frac{\gamma \mu_0 \nu}{4\pi r^2 \nu_{\text{NMR}}}$; $b = -\frac{\gamma \mu_0 \nu}{4\pi r^2 \nu_{\text{NMR}}} N + \frac{\gamma B_0}{\nu_{\text{NMR}}} - \frac{\nu_{\text{TMS}}}{\nu_{\text{NMR}}}$.

From the Eq. (9), chemical shift can be related to partial charge in a linear correlation manner. Indeed, the linear equation is the most proper relationship we have been tried. In this work, the linear mathematic model was built assess how well chemical shift is correlates with different type of partial charge.

Chemical shifts are therefore defined based on the same principle even the sensitivity of measurements is much lower for C-13 chemical shifts than that for the H-1 nucleus. Poor sensitivity of the magnetically active C-13 may result from the lower than 1.1% natural abundance, smaller gyromagnetic ratio, and J-coupling caused by hydrogen.

Concept of partial charges is used to rationalize material chemical properties. However, the partial charges cannot be observed from experiments due to the fact that electrons exhibit diffuse charge distributions with respect to nuclei. The partial charges can be derived from quantum mechanics wave functions following two approaches, orbital occupancy based method and spatial decomposition based method. The partitioning scheme for Mulliken partial charges is based on the total electron density basis functions of atomic center, and too basis-set-dependent to provide accurate assignment of partial charges [8]. The drawback of the Mulliken population scheme is particularly addressed in the natural population algorithm which assigns charges into atomic orbital on the basis of blocks of electron density matrix [50]. Therefore, inaccurate Mulliken partial charge is not appropriate for qualitative analysis, and is included in this work because it is calculated by default in the Gaussian-09 package. The NBO based natural population analysis (NPA) is relatively independent of basis set, so NBO charges of carbon atoms for 2-HADNT agree well with the experimental chemical shifts. The ESP defines charge for atomic center from the observable molecular electrostatic potential (MEP) of minimized structure on a three dimensional grid. The ESP partial charges feature slight conformational dependence, and the agreement with experimental chemical shifts may varies from many local minimum configurations [51].

From Fig. 5(a) it is found that among the commonly used three types of partial charges, the NBO charge demonstrates the strongest correlation (the coefficient of determination for linear regression $R^2 = 0.8512$) with the absolute chemical shifts for all the six aromatic and one non-aromatic carbon atom C₁₅. The correlation between the chemical shifts and the ESP charges is much weaker, as indicated by a much smaller R^2 of 0.2065. It can also be deduced from the nearly-zero R^2 (0.0542) that the absolute chemical shifts are almost not correlated with the MK charges.

The relationships between the relative chemical shifts of the six aromatic carbon atoms (compare to the chemical shifts of benzene carbon atoms) and the relative partial charges (compare to the partial charges of benzene ring) are illustrated in Fig. 5(b). Similar to Fig. 5(a), the strongest correlation ($R^2 = 0.7532$) occurs between the relative chemical shifts and relative NBO charges of the six phenyl ring carbon atoms. Different from Fig. 5(a), the correlation between the relative chemical shifts and the relative ESP charges is much stronger than the correlation between the absolute results and very close to that the correlation of the NBO charges ($R^2 = 0.7151$). Just as observed from Fig. 5(a), the correlation between the relative chemical shifts and the relative MK charges are the weakest but it is still much stronger than that between the absolute results ($R^2 = 0.4828$). Overall, the calculated NBO partial charges are most closely correlated with the experimental chemical shifts and the MK partial charges show least correlation with the experimental chemical shifts.

Conclusions

In summary, C-13 chemical shifts and atomic partial charges for 2-HADNT are calculated using MP2 and seven DFT methods in this study. The C-13 chemical shifts are also determined experimentally. As observed from the analysis results, the MP2 calculation provides the most accurate C-13 chemical shifts of 2-HADNT by comparing with experimental data for this highly correlated nitro-aromatic compound. It indicates the importance of considering correlation forces in the calculations of chemical shifts for highly correlated nitro-aromatic system. Furthermore, O3LYP method gives the most accurate predictions of chemical shifts among the seven DFT methods with the same correlation functional. The average deviations of the calculated chemical shifts using O3LYP from the experimental data is very close to those using MP2. It is therefore possible to achieve reasonable calculated chemical shifts for compounds with conjugated π system when an appropriate DFT method is selected. The NBO partial charges yielded from MP2 calculations represent the electron density distributions of 2-HADNT more accurately than both ESP and MK charges. The present work can be further verified using CCSD(T) method, a higher level method than MP2. This work is very helpful in the development of new DFT methods using the electron density derived from NBO partial charges and experimental chemical shifts.

Acknowledgments

The authors are grateful for the support provided through the Department of Chemistry, University of Louisiana at Lafayette. All QM calculations were conducted using a quad-core cluster canpe01 and a dual-core canfire04. All the high performance computational resources used for this work were provided by the Louisiana Optical Network Initiative (<http://www.loni.org>).

References

- [1] T. Helgaker, M. Jaszunski, K. Ruud, *Chem. Rev.* 99 (1999) 293–352.
- [2] L.B. Casabianca, A.C. de Dios, *J. Chem. Phys.* 128 (2008) 2816784.
- [3] F.A. Mulder, M. Filatov, *Chem. Soc. Rev.* 39 (2010) 578–590.
- [4] H. Sun, L.K. Sanders, E. Oldfield, *J. Am. Chem. Soc.* 124 (2002) 5486–5495.
- [5] A. Perczel, A.G. Császár, *J. Comput. Chem.* 21 (2000) 882–900.
- [6] G. Magyarfalvi, P. Pulay, *J. Chem. Phys.* 119 (2003) 1350–1357.
- [7] J.C. Facelli, *Concepts Magn. Reson. Part A* 20A (2004) 42–69.
- [8] D. Cremer, L. Olsson, F. Reichel, E. Kraka, *Isr. J. Chem.* 33 (1993) 369–385.
- [9] H.-U. Siehl, T. Müller, J. Gauss, *J. Phys. Org. Chem.* 16 (2003) 577–581.
- [10] H.-U. Siehl, T. Müller, J. Gauss, *J. Phys. Org. Chem.* 16 (2003) 880–880.
- [11] F. Nozairov, T. Kupka, M. Stachów, *J. Chem. Phys.* 140 (2014).
- [12] K. Friedrich, G. Seifert, G. Großmann, *Z Phys. D – Atoms, Mol. Clusters* 17 (1990) 45–46.
- [13] R. Ditchfield, W.J. Hehre, J.A. Pople, *J. Chem. Phys.* 54 (1971) 724–728.

- [14] V.G. Malkin, O.L. Malkina, D.R. Salahub, *Chem. Phys. Lett.* 204 (1993) 87–95.
- [15] M. Schindler, W. Kutzelnigg, *J. Am. Chem. Soc.* 105 (1983) 1360–1370.
- [16] A.E. Hansen, T.D. Bouman, *J. Chem. Phys.* 82 (1985) 5035–5047.
- [17] T.A. Keith, R.F.W. Bader, *Chem. Phys. Lett.* 210 (1993) 223–231.
- [18] T.A. Keith, R.F.W. Bader, *Chem. Phys. Lett.* 194 (1992) 1–8.
- [19] K. Wolinski, J.F. Hinton, P. Pulay, *J. Am. Chem. Soc.* 112 (1990) 8251–8260.
- [20] J. Gauss, *Chem. Phys. Lett.* 191 (1992) 614–620.
- [21] G. Rasul, G.K.S. Prakash, G.A. Olah, *Proc. Natl. Acad. Sci. USA* 99 (2002) 9635–9638.
- [22] G. Rasul, G.K.S. Prakash, G.A. Olah, *J. Phys. Chem. A* 110 (2005) 1041–1045.
- [23] C. van Wüllen, W. Kutzelnigg, *J. Chem. Phys.* 104 (1996) 2330–2340.
- [24] J. Gauss, J.F. Stanton, *J. Chem. Phys.* 103 (1995) 3561–3577.
- [25] D.-D. Yang, F. Wang, J. Guo, *Chem. Phys. Lett.* 531 (2012) 236–241.
- [26] G. Rasul, G.K.S. Prakash, G.A. Olah, *J. Phys. Chem. A* 117 (2013) 4664–4668.
- [27] K.L. Bak, P. Jørgensen, J. Olsen, T. Helgaker, J. Gauss, *Chem. Phys. Lett.* 317 (2000) 116–122.
- [28] J. Gauss, J.F. Stanton, *J. Chem. Phys.* 104 (1996) 2574–2583.
- [29] G. Colherinhas, T.L. Fonseca, M.A. Castro, *Chem. Phys. Lett.* 503 (2011) 191–196.
- [30] T. Rohmer, J. Matysik, F. Mark, *J. Phys. Chem. A* 115 (2011) 11696–11714.
- [31] G. Schreckenbach, T. Ziegler, *J. Phys. Chem.* 99 (1995) 606–611.
- [32] M. Bühl, *Chem. Phys. Lett.* 267 (1997) 251–257.
- [33] G. Vignale, M. Rasolt, *Phys. Rev. B* 37 (1988) 10685–10696.
- [34] P.J. Wilson, R.D. Amos, N.C. Handy, *Chem. Phys. Lett.* 312 (1999) 475–484.
- [35] P.v.R. Schleyer, H. Jiao, N.J.R.v.E. Hommes, V.G. Malkin, O.L. Malkina, *J. Am. Chem. Soc.* 119 (1997) 12669–12670.
- [36] A.D. Becke, *Phys. Rev. A* 38 (1988) 3098–3100.
- [37] C. Lee, W. Yang, R.G. Parr, *Phys. Rev. B* 37 (1988) 785–789.
- [38] X. Xu, W.A. Goddard, *J. Phys. Chem. A* 108 (2004) 8495–8504.
- [39] J. Baker, P. Pulay, *J. Chem. Phys.* 117 (2002) 1441–1449.
- [40] J.H. Gardner, E.M. Purcell, *Phys. Rev.* 76 (1949) 1262–1263.
- [41] N.A. Ogorodnikova, A.A. Koridze, É.I. Fedin, P.V. Petrovskii, *Russ. Chem. Bull.* 32 (1983) 1847–1850.
- [42] K. Matsumoto, M. Ciobanu, K. Aoyama, T. Uchida, *Heterocycl. Commun.* 3 (1997) 499.
- [43] T. Junk, W.J. Catallo, *Chem. Speciation Bioavailability* 10 (1998) 47–52.
- [44] M.J. Frisch, G.W. Trucks, H.B. Schlegel, G.E. Scuseria, M.A. Robb, J.R. Cheeseman, G. Scalmani, V. Barone, B. Mennucci, G.A. Petersson, H. Nakatsuji, M. Caricato, X. Li, H.P. Hratchian, A.F. Izmaylov, J. Bloino, G. Zheng, J.L. Sonnenberg, M. Hada, M. Ehara, K. Toyota, R. Fukuda, J. Hasegawa, M. Ishida, T. Nakajima, Y. Honda, O. Kitao, H. Nakai, T. Vreven, J. Montgomery, J.A., J.E. Peralta, F. Ogliaro, M. Bearpark, J.J. Heyd, E. Brothers, K.N. Kudin, V.N. Staroverov, R. Kobayashi, J. Normand, K. Raghavachari, A. Rendell, J.C. Burant, S.S. Iyengar, J. Tomasi, M. Cossi, N. Rega, J.M. Millam, M. Klene, J.E. Knox, J.B. Cross, V. Bakken, C. Adamo, J. Jaramillo, R. Gomperts, R.E. Stratmann, O. Yazyev, A.J. Austin, R. Cammi, C. Pomelli, J.W. Ochterski, R.L. Martin, K. Morokuma, V.G. Zakrzewski, G.A. Voth, P. Salvador, J.J. Dannenberg, S. Dapprich, A.D. Daniels, Ö. Farkas, J.B. Foresman, J.V. Ortiz, J. Cioslowski, D.J. Fox, *Gaussian 09 Revision A.1*, Gaussian Inc., Wallingford, CT, USA, 2009.
- [45] A.V. Marenich, C.J. Cramer, D.G. Truhlar, *J. Phys. Chem. B* 113 (2009) 6378–6396.
- [46] J. Baker, P. Pulay, *J. Comput. Chem.* 24 (2003) 1184–1191.
- [47] T.W. Keal, D.J. Tozer, T. Helgaker, *Chem. Phys. Lett.* 391 (2004) 374–379.
- [48] D.B. Chesnut, *Chem. Phys. Lett.* 380 (2003) 251–257.
- [49] M.A. Watson, N.C. Handy, A.J. Cohen, T. Helgaker, *J. Chem. Phys.* 120 (2004) 7252–7261.
- [50] R.F.W. Bader, *Chem. Rev.* 91 (1991) 893–928.
- [51] M. Basma, S. Sundara, D. Çalgan, T. Vernali, R.J. Woods, *J. Comput. Chem.* 22 (2001) 1125–1137.
- [52] D. Graham, A.R. Kennedy, C.J. McHugh, W.E. Smith, W.I.F. David, K. Shankland, N. Shankland, *New J. Chem.* 28 (2004) 161–165.
- [53] T. Junk, Y.-M. Liu, Z. Li, R. Perkins, Y.-C. Liu, *J. Mol. Struct.* 1080 (2015) 145–152.